International Journal of the Physical Sciences Vol. 6(33), pp. 7456 - 7470, 9 December, 2011
Available online at http://www.academicjournals.org/IJPS
DOI: 10.5897/IJPS11.1092
ISSN 1992 - 1950 © 2011 Academic Journals

Full Length Research Paper

Numerical study of laminar mixed convection heat transfer of power-law non-Newtonian fluids in square enclosures by finite volume method

Mohammad Reza Safaei[1]*, Behnam Rahmanian[2] and Marjan Goodarzi[3]

[1]Young Researchers Club and Department of Mechanical Engineering, Mashhad Branch, Islamic Azad University, Mashhad, Iran.
[2]Department of Mechanical Engineering, Mashhad Branch, Islamic Azad University, Mashhad, Iran.
[3]Department of Computer Engineering, Mashhad Branch, Islamic Azad University, Mashhad, Iran.

Accepted 23 October, 2011

In this study, we have numerically considered mixed convection heat transfer in a square enclosure with cold left and right walls, insulated moving upper wall and hot fixed lower wall. The governing flows of two reliable articles were initially modeled and after validating calculations, the given flow of the study was solved by finite volume method. To examine the effects of different factors, such as Prandtl, Reynolds and Rayleigh numbers on heat transfer in a square enclosure, the laminar flow of Newtonian fluids was approximated and then laminar flow of non-Newtonian fluids, such as carboxy methyl cellulose (CMC) and carboxy poly methylene (Carbopol) water solutions were studied for different Richardson numbers. It was found from the results obtained in the present study that when Ri is less than 1, governing heat transfer inside the enclosure is forced convection for non-Newtonian fluids similar to Newtonian ones. When Ri increases, the effect of forced convection is reduced and natural convection heat transfer increases. It was also found that in constant Grashof numbers, if *n* decreases, the dimensionless temperature increases. Also, if *n* is constant, any increase in Grashof number causes a higher dimensionless temperature. It may be related to the fact that in similar conditions, any increase in forced convection, makes shear stresses more.

Key words: Richardson number, power-law non-Newtonian fluids, mixed convection heat transfer, square enclosure, finite volume method.

INTRODUCTION

The process of heat transfer, in which the free convection and forced convection occur coincidentally, is called mixed convention heat transfer. Mixed convection heat transfer occurs when the buoyancy effect in a forced flow or the effect of forced flow in a buoyancy flow is significant (Safaei and Goshayeshi, 2010).

In recent years, the practical applications of mixed convection heat transfer in various areas such as designing solar collectors, double-layer glasses, building insulation, cooling electronic parts, food drying, sterilization, etc., have motivated many scientists to study this phenomenon.

Basak et al. (2009) have studied laminar mixed convection of airflow inside a square enclosure by using a finite element method. Using local Nusselt number, they showed that the rate of heat transfer on the corners of the lower wall is high and decreases on its center.

Oztop and Dagtekin (2004) conducted a study on laminar mixed convection flow inside an enclosure with moving isothermal vertical and insulated horizontal walls. They examined the flow of air (Pr = 0.7) in Gr = 10^4 and 0.01 < Ri < 100. The results of his study demonstrated that in low values of Richardson's number, if the moving

*Corresponding author. E-mail: CFD_Safaiy@yahoo.com. Tel: +98 9151022063.

walls of the enclosure move inversely, the heat transfer from the enclosure is more than the state that walls slide on one direction.

On the other hand, since a long time ago, the behavior of fluids and their characteristics have been focused. Considering the linear relation between the changes in shear stress and rate of shear strain, the behavior of many single-phase fluids which include merely the compounds with low molecular weight has been simulated. These fluids are called Newtonian fluids. The development of chemical industry at the beginning of the 20th century resulted in emergence of an expansive spectrum of synthetic materials, such as polymers. Moreover, increasing the usage of materials such as suspensions, emulsions, adhesives and the advent of oil exploration required to study a variety of materials which show strange behavior, because the relations of Newtonian fluids was not able to predict their shear behavior. The flow behavior of these fluids, called non-Newtonian fluids, cannot be described by Newtonian model. Therefore, other models of flow behavior have been presented for these fluids which are extensively used in computer simulations (Maghmoumi, 2008; Alavi et al., 2008).

Considering the studies done by the other scientists, it was found that, unfortunately, there is no certain article about mixed convection heat transfer inside enclosures by using non-Newtonian fluids and most of the conducted researches are about natural convection heat transfer inside enclosures.

Demir and Akyoldoz (2000) solved laminar natural convection problem of a visco-elastic non-Newtonian fluid inside a square enclosure by using a finite difference method inside a square enclosure. They studied the effect of Weissenberg number (which is the criterion for the elasticity rate of fluid) and Rayleigh number on profiles of temperature and streamlines. They found that for their geometry, $We_{critical}$ is 0.1 and in Weissenberg numbers more than this value, the system becomes unstable and its equilibrium is lost. Of course, with consideration to the specificity of their fluid, their study is continuing experimentally and numerically. They try to describe the bifurcation phenomena for such variety of fluids in near future.

Kim et al. (2003) studied laminar free convection of a power-law fluid inside a square enclosure with insulated upper and lower walls, cold left wall and hot right wall. They conducted numerical and scale analysis for fluids such as carboxy poly methylene (Carbopol) and carboxy methyl cellulose (CMC) in $10^5 < Ra < 10^7$. Findings of this research showed that for high Rayleigh number and medium Prandtl number, if n decreases, the convection activity increases and total heat transfer augments, while when Rayleigh number and Prandtl number increase, Rheological properties of the fluid have significant effect on both stable and transient flows.

Lamsaadi et al. (2006) studied laminar natural convection of power-law non-Newtonian fluid inside a rectangular enclosure with adiabatic long horizontal walls and variable-thermal-flux vertical walls by approximate theoretical solution and numerical method. In this research, they used a non-Newtonian fluid consisting of 4% paper pulp in water. In this study AR = 8, $0 < Ra < 10^6$ and $0.6 < n < 1.4$ were considered. It was found from the comparison between the numerical results and analytical solution that fluid flow and characteristics of heat transfer for non-Newtonian fluid is more sensitive than Newtonian fluid; in such a way, shear thinning fluid ($0 < n < 1$), the rate of convection heat transfer and recirculation increases; while shear-thickening fluid ($n > 1$) has an inverse effect. It was also found that in higher Prandtl numbers, natural convection inside the enclosure is controlled only by Rayleigh number and n.

In one of most recent works, Turan et al. (2010) have studied laminar natural convection inside a square enclosure filled with Bingham fluids. In their studied enclosure, the left, right, upper and lower walls were hot, cold and insulated, respectively. The ranges of Rayleigh and Prandtl numbers studied by them were 10^3 to 10^6 and 0.1 to 100, correspondingly. As indicated in their study, when Rayleigh number (Ra) increases, Nusselt number (Nu) also augments for Newtonian and non-Newtonian fluids. Although, in similar conditions, Nu is less for non-Newtonian fluid.

In the present paper, firstly, mixed convection heat transfer of air inside a square enclosure which has already been studied by Basak et al. (2009) and Oztop and Dagtekin (2004) was solved and after proving the accuracy of the solution, the laminar flow inside the square enclosure was studied by water and several other power-law non-Newtonian fluids for studying the rheological effect of fluids on mixed convection inside the enclosure, so that the effect of these properties on mixed convection heat transfer is realized for the first time in the world.

GOVERNING EQUATIONS IN TWO-DIMENSIONAL STATE

The continuity, energy and momentum equations have been studied for modeling this flow. The viscosity has been calculated through power-law. The density has been computed by employing Boussinesq approximation for $\Delta T < 30^{\circ}C$ and variable density parameter for $\Delta T > 30^{\circ}C$. The other characteristics have been considered constant.

The governing equations are as follows (Maghmoumi, 2008):

Continuity equation:

$$\frac{\partial \rho}{\partial t} + \frac{\partial u}{\partial x} + \frac{\partial v}{\partial y} = 0 \qquad (1)$$

Table 1. Characteristics of non-Newtonian fluids (Chhabra, 2007; Maghmoumi, 2008).

Name	Temperature (K)	n	m (Pa.sn)	Shear rate (s-1)
0.125% Carbopol	290	0.32	6.67	1-100
0.09% Carbopol	290	0.44	2.37	1-100
0.05% Carbopol	290	0.65	0.1103	1-100
0.77% carboxymethyl cellulose	294	0.95	0.044	44-560
Water	305	1	0.000769	1-100
Ideal fluid	305	1	1	1-100

Momentum equation in X Direction:

$$\rho\left(\frac{\partial u^2}{\partial x}+\frac{\partial uv}{\partial y}\right)=-\frac{\partial P}{\partial x}+\frac{\partial}{\partial x}\left[\eta_{xx}\frac{\partial u}{\partial x}\right]+\frac{\partial}{\partial y}\left[\eta_{yx}\frac{\partial u}{\partial y}\right]+\rho g_x \quad (2)$$

Momentum equation in Y Direction:

$$\rho\left(\frac{\partial uv}{\partial x}+\frac{\partial v^2}{\partial y}\right)=-\frac{\partial P}{\partial y}+\frac{\partial}{\partial x}\left[\eta_{xy}\frac{\partial v}{\partial x}\right]+\frac{\partial}{\partial y}\left[\eta_{yy}\frac{\partial v}{\partial y}\right]+\rho g_y \quad (3)$$

where:

$$\eta_{xx}=\left|m\left(\frac{\partial u}{\partial x}\right)^{n-1}\right| \quad (4)$$

$$\eta_{yx}=\left|m\left(\frac{\partial u}{\partial y}\right)^{n-1}\right| \quad (5)$$

$$\eta_{xy}=\left|m\left(\frac{\partial v}{\partial x}\right)^{n-1}\right| \quad (6)$$

$$\eta_{yy}=\left|m\left(\frac{\partial v}{\partial y}\right)^{n-1}\right| \quad (7)$$

Energy equation:

$$\frac{\partial T}{\partial t}+u\frac{\partial T}{\partial x}+v\frac{\partial T}{\partial y}=\alpha\left(\frac{\partial^2 T}{\partial x^2}+\frac{\partial^2 T}{\partial y^2}\right) \quad (8)$$

In the recent equation, m and n which are called constitutive parameters are two experimental parameters. The value of n varies between 0 and 1 for a shear-thinning fluid. As much as the value of n is less, the shear-thinning property of fluid is more.

Table 1 shows the characteristics of non-Newtonian fluids used in the present study. The ideal fluid used in this study (m = 1, n = 1) is an assumptive fluid and will be employed for better comparison of the results.

The schematic used in this study has been illustrated in Figure 1. The boundary conditions have also been shown on this figure.

These boundary conditions are as follows:

$0 \le x \le L$ and $y = 0$ $T=T_H$ (9)

$0 \le x \le L$ and $y = L$,u= U_0 and $\frac{\partial T}{\partial y}=0$ (10)

$0 \le y \le L$ aT= T_C (11)

$0 \le y \le L$ and $x = 0$ $T=T_C$ (12)

In this case, the stream function is calculated as follows:

$$v=-\frac{\partial \psi}{\partial x} \text{ and } u=\frac{\partial \psi}{\partial y} \quad (13)$$

NUMERICAL SOLUTION METHOD

Finite volume method, described in details (Patankar, 1980; Goshayeshi et al., Safaei and Maghmoumi, 2009; Safaei, 2009) has been used for solving the governing differential equations on the flow. In this method, the calculation domain has been divided into several control volumes in such a way that any node is surrounded by a control volume and the control volumes have no shared volume.

The integration of the differential equation on any of the control volumes was obtained. The piece-by-piece profile that indicates the changes of ϕ (an optional quantity such as temperature, velocity, etc.) between nodes, have been used for integrations. The result is discretization equation that includes values of ϕ for a group of nodes (Patankar, 1980).

The convection and the diffusion terms discretization methods are

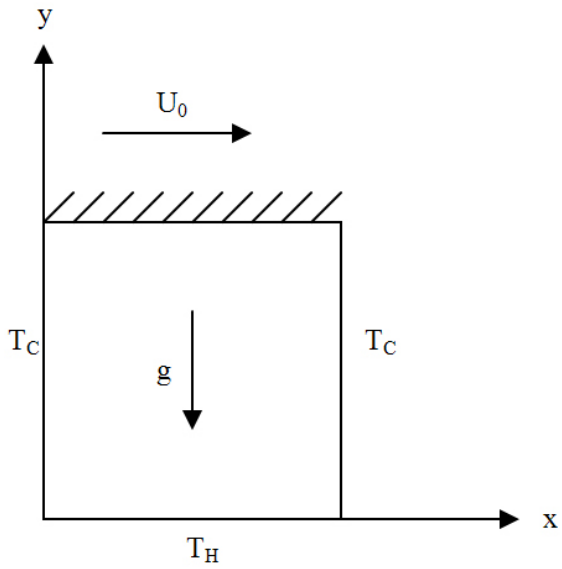

Figure 1. Schematic of the problem.

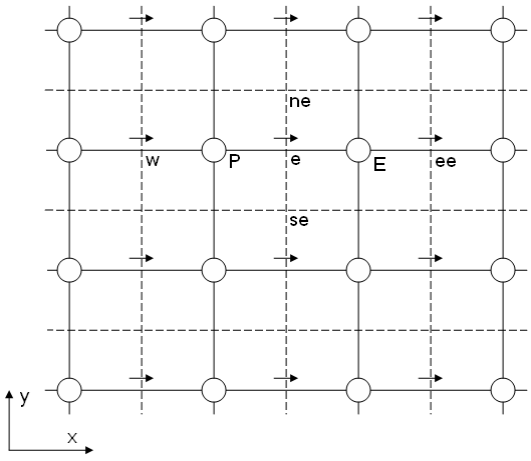

Figure 2. Staggered location for u.

hybrid and second order central difference schemes, respectively. Upon the correlation of Buoyancy term (Momentum equation to the direction of y) with the temperature, the governing equations are coupled and have to be solved simultaneously. In the momentum equations, the pressure term is achieved through the use of simple algorithm and it is calculated in a way that the continuity equation is valid. The resulting algebraic system of equations is solved by using implicit line-by-line tri diagonal-matrix algorithm. The convergence of the solution is only accepted when the absolute maximum value of conservation of energy is less than 10^{-7}. Such remaining amount guarantees the validity of this study.

Discretization equations for two dimensions

Now, by taking into consideration the first order upwind scheme, the discretization equations could be written as follows; for example, for velocity equation in X direction and staggered location for u (Figure 2), we have (Patankar, 1980; Maghmoumi, 2008):

$$u_e.A_e = A_{ne}.u_{ne} + A_{se}.u_{se} + A_{ee}.u_{ee} + A_w.u_w + (P_p - P_E).\Delta y$$

In which the coefficients are obtained as follows:

$$A_{ne} = D_{ne} + Max(-F_{ne}, 0) \quad (15)$$

$$A_{se} = D_{se} + Max(0, F_{se}) \quad (16)$$

$$A_{ee} = D_{ee} + Max(-F_{ee}, 0) \quad (17)$$

$$A_w = D_w + Max(0, F_w) \quad (18)$$

$$A_e = A_e + A_{se} + A_{ee} + A_w \quad (19)$$

where D and F are defined as follows:

$$D_{ne} = G_{ne}.\frac{\Delta x}{\delta y} \quad (20)$$

$$D_{se} = G_{se}.\frac{\Delta x}{\delta y} \quad (21)$$

$$D_w = G_w.\frac{\Delta y}{\delta x} \quad (22)$$

$$D_{ee} = G_{ee}.\frac{\Delta y}{\delta x} \quad (23)$$

$$F_{ne} = \rho V_{ne}.\Delta y \quad (24)$$

$$F_{se} = \rho V_{se}.\Delta y \quad (25)$$

$$F_w = \rho V_w.\Delta x \quad (26)$$

$$F_{ee} = \rho V_{ee}.\Delta x \quad (27)$$

$$G_{ne} = m\left|\frac{u_{ne} - u_e}{\Delta y}\right|^{n-1} \quad (28)$$

$$G_{se} = m\left|\frac{u_e - u_{se}}{\Delta y}\right|^{n-1} \quad (29)$$

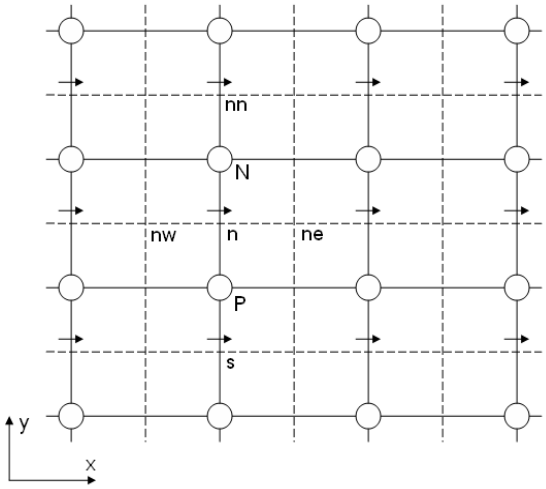

Figure 3. Staggered location for v.

$$G_w = m\left|\frac{u_e - u_w}{\Delta x}\right|^{n-1} \quad (30)$$

$$G_{ee} = m\left|\frac{u_{ee} - u_e}{\Delta x}\right|^{n-1} \quad (31)$$

$$du_n = \frac{\Delta y}{A_e} \quad (32)$$

For velocity equation in Y direction and staggered location for v (Figure 3), we also have:

$$v_n.A_n = A_{nn}.v_{nn} + A_{ne}.v_{ne} + A_{nw}.v_{nw} + A_s.v_s + (p_p - p_N).\Delta x \quad (33)$$

$$A_{nn} = D_{nn} + Max(-F_{nn}, 0) \quad (34)$$

$$A_{ne} = D_{ne} + Max(-F_{ne}, 0) \quad (35)$$

$$A_{nw} = D_{nw} + Max(0, F_{nw}) \quad (36)$$

$$A_s = D_s + Max(0, F_s) \quad (37)$$

$$A_n = A_s + A_{nw} + A_{ne} + A_{nn} \quad (38)$$

$$D_{nn} = G_{nn}.\frac{\Delta x}{\delta y} \quad (39)$$

$$D_{ne} = G_{ne}.\frac{\Delta y}{\delta x} \quad (40)$$

$$D_{nw} = G_{nw}.\frac{\Delta y}{\delta x} \quad (41)$$

$$D_s = G_s.\frac{\Delta x}{\delta y} \quad (42)$$

$$F_{nn} = \rho V_{nn}.\Delta y \quad (43)$$

$$F_{ne} = \rho V_{ne}.\Delta x \quad (44)$$

$$F_{nw} = \rho V_{nw}.\Delta x \quad (45)$$

$$F_s = \rho V_s.\Delta y \quad (46)$$

$$G_{nn} = m\left|\frac{v_{nn} - v_n}{\Delta y}\right|^{n-1} \quad (47)$$

$$G_{ne} = m\left|\frac{v_{ne} - v_n}{\Delta x}\right|^{n-1} \quad (48)$$

$$G_{nw} = m\left|\frac{v_n - v_{nw}}{\Delta x}\right|^{n-1} \quad (49)$$

$$G_s = m\left|\frac{v_n - v_s}{\Delta y}\right|^{n-1} \quad (50)$$

Pressure-correction equation:

$$a_P P'_P = a_E P'_E + a_W P'_W + a_N P'_N + a_S P'_S + b \quad (51)$$

$$a_p = a_e + a_w + a_n + a_s \quad (52)$$

$$a_E = \rho.\Delta y.d_e \quad (53)$$

$$a_W = \rho.\Delta y.d_W \quad (54)$$

$$a_N = \rho.\Delta x.d_n \quad (55)$$

$$a_S = \rho.\Delta x.d_s \quad (56)$$

$$b = \rho.\Delta x(v_s - v_n) + \rho.\Delta y(u_w - u_e) \quad (57)$$

$$p = p^* + \alpha_p.p' \quad (58)$$

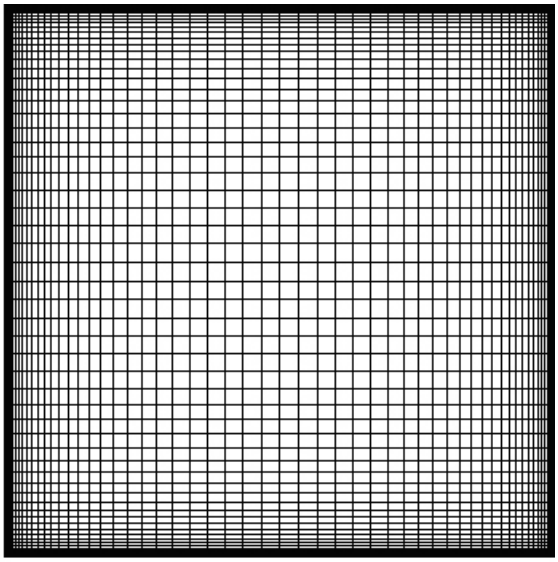

Figure 4. One of the grids used in the present study.

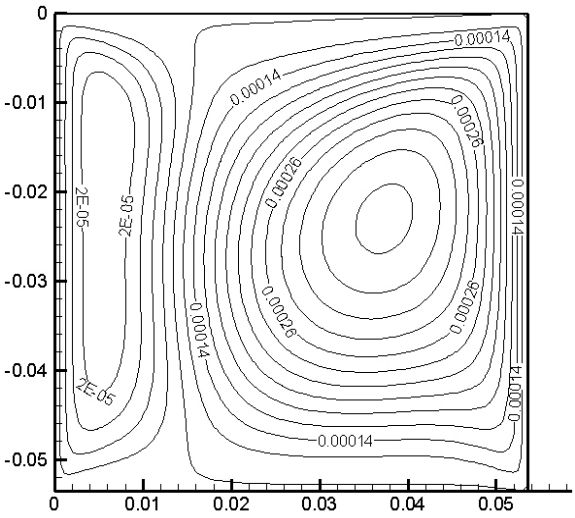

Figure 6. Stream function with Ri = 1, in comparison with Oztop and Dagtekin (2004).

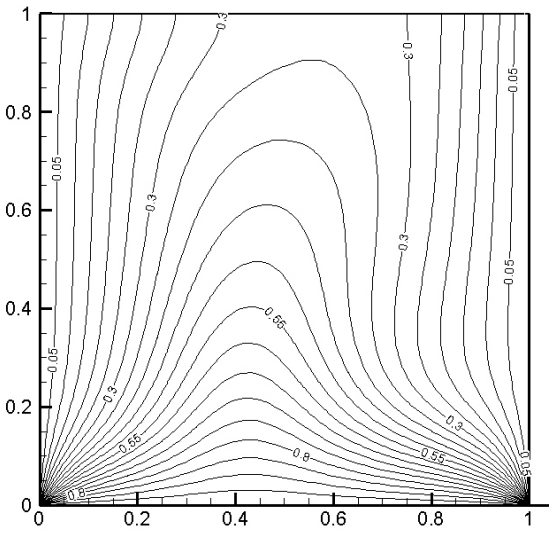

Figure 5. Temperature contour with Ri = 100, in comparison with Basak et al. (2009).

where α_p is under relaxation factor to determine the pressure and is usually chosen to be less than 0.6. In addition, other coefficients for discretization of the given point are obtained with the help of the aforementioned equations.

RESULTS

Grid generation and grid independence

The grid generation in this study is an algebraic method. Instead of using a mesh with uniform distribution in the physical domain, the mesh points can get congested in the regions with high gradient which can result in decrease of the total number of meshes as well as increasing the efficiency of problem solving. This type of mesh is convenient to solve the calculations related to boundary layer.

Figure 4 shows one of the grids used in the present study.

Studying Newtonian mixed convection inside a square enclosure

In laminar state, Gr = 10^4 and Pr = 0.7 is considered constant for comparison with the results obtained from Basak et al. (2009) and Oztop and Dagtekin (2004), where 0.01 < Re < 100 has changed. Figures 5 and 6 demonstrate the contours of temperature and stream function in comparison with Basak et al. (2009) and Oztop and Dagtekin (2004). The suitable agreement of these contours indicates the accuracy of the problem solution in this study.

Next, the aforementioned problem has been solved with the same boundary conditions but through the use of non-Newtonian fluids.

Studying laminar flow of non-Newtonian fluids

Figures 7 and 8 are diagrams of the dimensionless temperature in the mid-height for various kinds of non-Newtonian fluids. It was found from the diagrams that Grashof number and power-law index have significant influences on characteristics of heat transfer; in such a way that in constant Grashof, any decrease in n results in

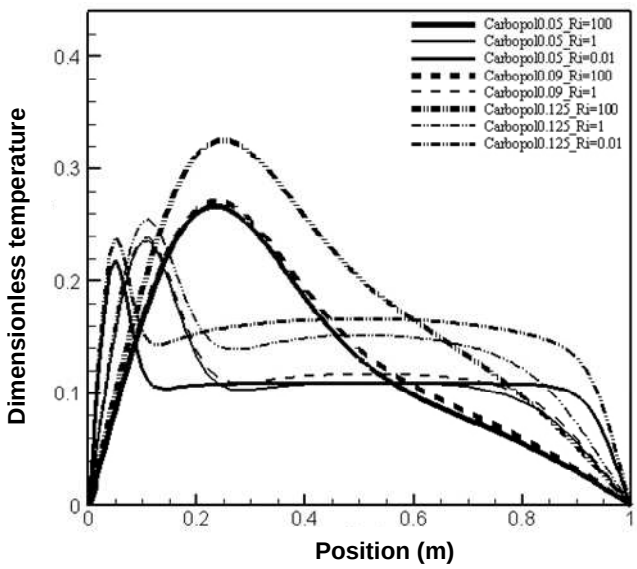

Figure 7. Dimensionless temperature in the mid-height for Carbopol in different concentrations.

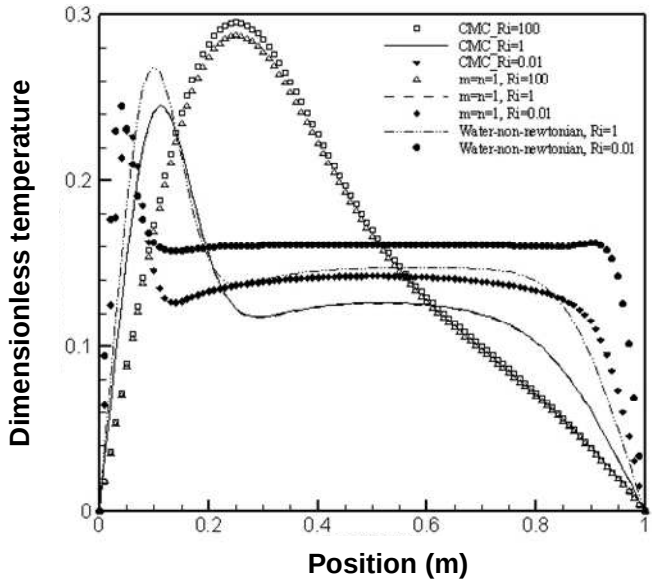

Figure 8. Dimensionless temperature in the mid-height for water, CMC and ideal flow.

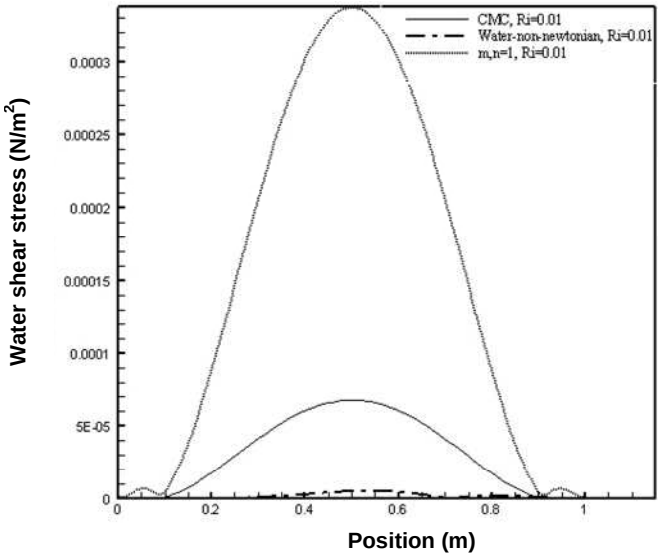

Figure 9. Wall shear stress diagram alongside the hot lower wall and Ri = 0.01 for water, CMC and ideal fluid.

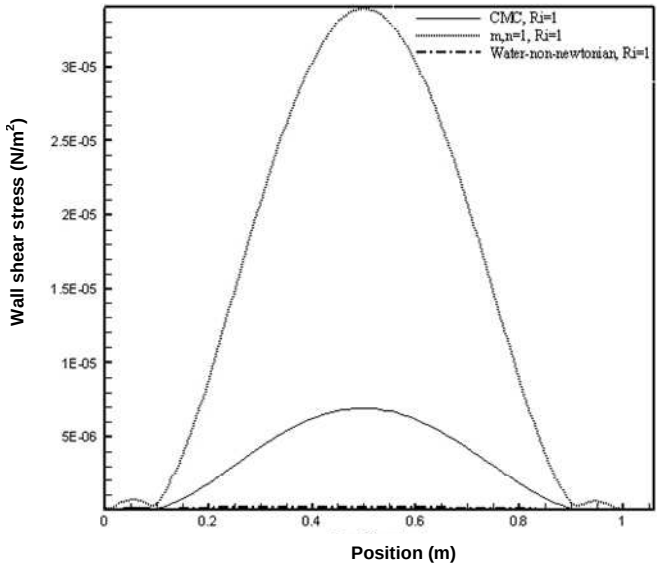

Figure 10. Wall shear stress diagram alongside the hot lower wall and Ri = 1 for water, CMC and ideal fluid.

increasing the dimensionless temperature; this is similar with the behavior for constant n in which Gr increases.

Figures 9 to 12 are diagrams of wall shear stress on lower wall for different non-Newtonian fluids and Richardson numbers.

As shown in the diagrams, when forced convection is governed, for all the non-Newtonian fluids, shear stress is about 10 folds of similar values in mixed convection. The value of shear stress, when natural convection is governed, is about 0.1 of the same value in mixed convection that indicates the effect of velocity of the higher wall on heat transfer inside the enclosures. The aforementioned diagrams also illustrates that in all Richardson numbers, the maximum values of shear stress is related to the ideal fluid with n = 1 and m = 1 and the minimum of these stresses is associate with

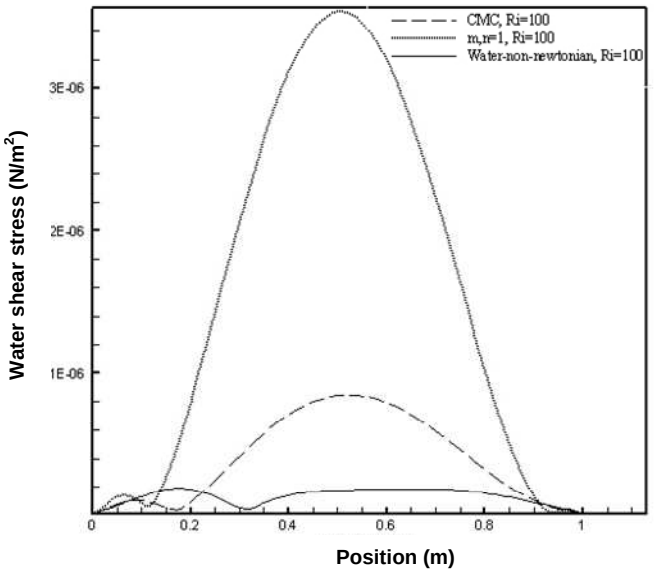

Figure 11. Wall shear stress diagram alongside the hot lower wall and Ri = 100 for water, CMC and ideal fluid.

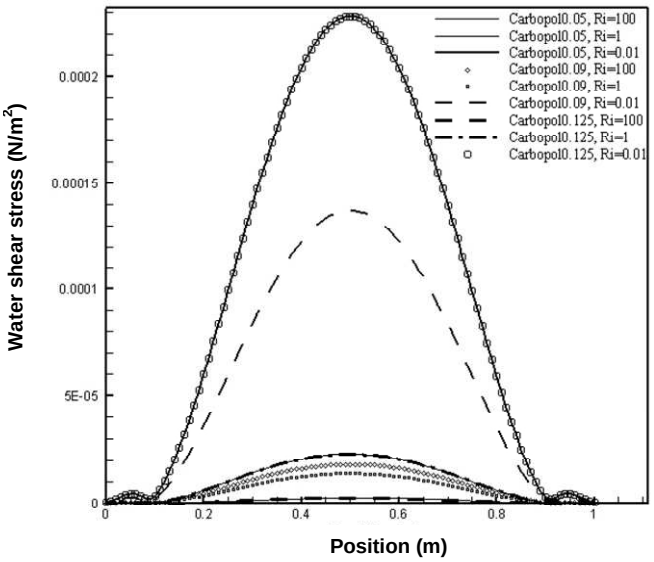

Figure 13. Wall shear stress diagram alongside the hot lower wall and Carbopol fluid with different concentrations.

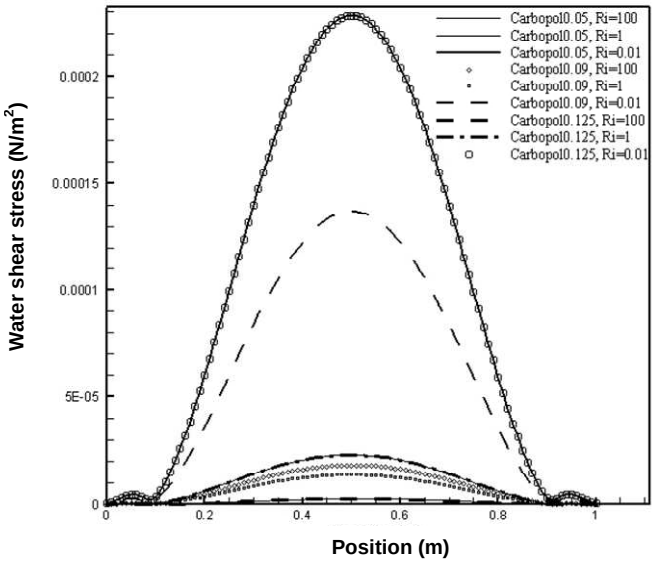

Figure 12. Wall shear stress diagram alongside the hot lower wall and Carbopol fluid with different concentrations.

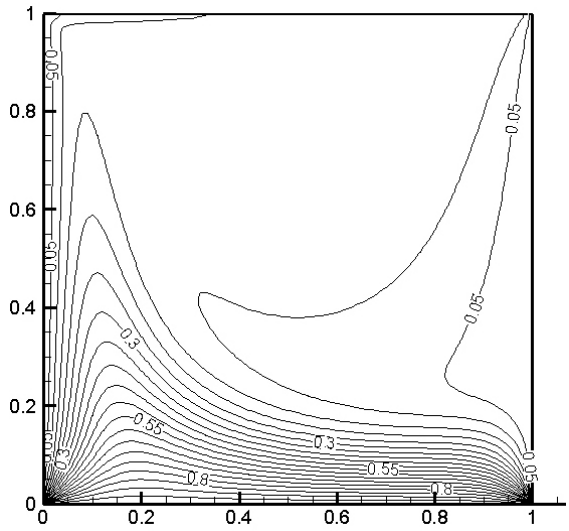

Figure 14. Dimensionless temperature contour for Carbopol 0.05% fluid in Ri = 1.

water. It should be reminded that water is a Newtonian fluid and in this study, it has been solved merely for comparing it with other non-Newtonian fluids by using the formulas of non-Newtonian fluids but with n = 1 and m = μ_{water}.

In Carbopol fluid, the concentrations 0.05 and 0.125% (n = 0.32 and n = 0.65) have maximum shear stress and the concentration 0.09% (n = 0.44) has minimum shear stress. However, in Ri = 100, it is on the contrary, that is, n = 0.44 has maximum and n = 0.32, n = 0.65 minimum shear stress.

Figures 13 to 30 show the contours of dimensionless temperature for different non-Newtonian fluids and water (as a Newtonian fluid) in 0.01 < Ri < 100. It is found that in governing natural convection, the isothermal lines are nearly symmetric and through transiting to forced convection, these lines become asymmetric. This is because the velocity is in higher wall of the enclosure. Since the flow is inside the enclosure, heat distribution is

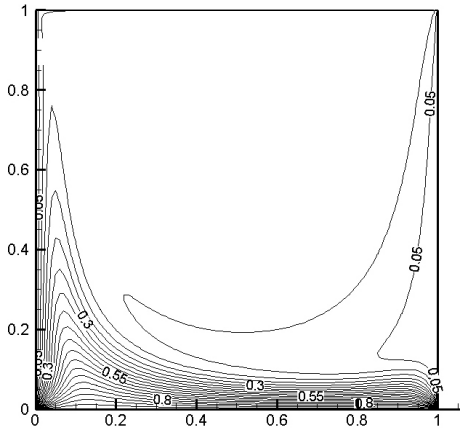

Figure 15. Dimensionless temperature contour for Carbopol 0.05% fluid in Ri = 0.01.

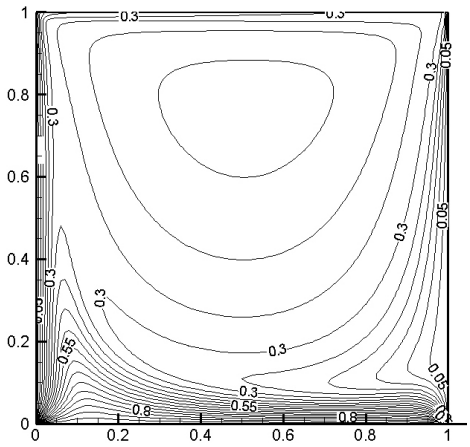

Figure 18. Dimensionless temperature contour for Carbopol 0.09% fluid in Ri = 0.01.

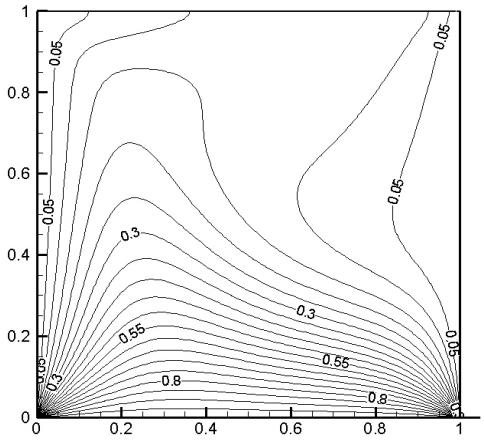

Figure 16. Dimensionless temperature contour for Carbopol 0.09% fluid in Ri = 100.

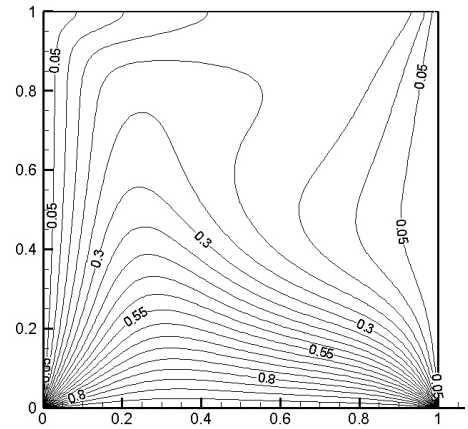

Figure 19. Dimensionless temperature contour for Carbopol 125 fluid in Ri = 100.

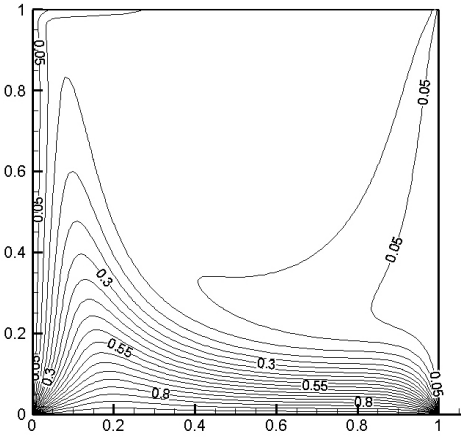

Figure 17. Dimensionless temperature contour for Carbopol 0.09% fluid in Ri = 1

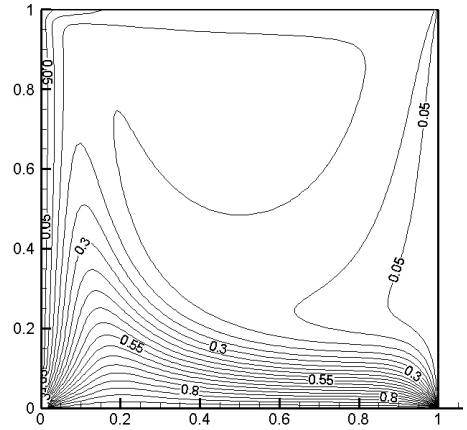

Figure 20. Dimensionless temperature contour for Carbopol 125 fluid in Ri = 1.

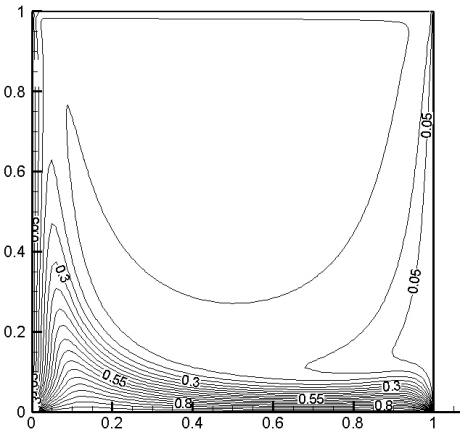

Figure 21. Dimensionless temperature contour for Carbopol 125 fluid in Ri = 0.01.

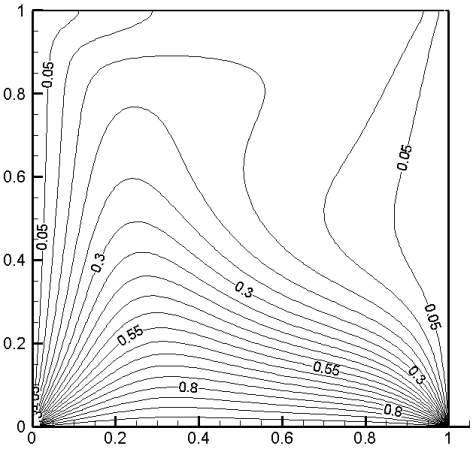

Figure 22. Dimensionless temperature contour for CMC fluid in Ri = 100.

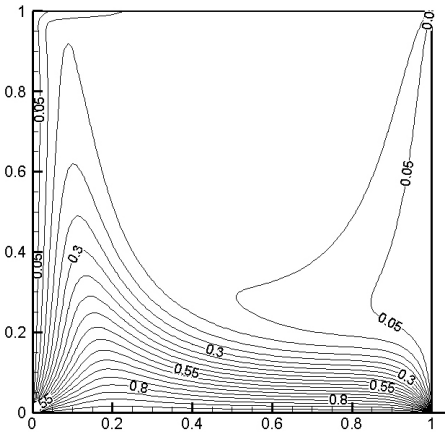

Figure 23. Dimensionless temperature contour for CMC fluid in Ri = 1.

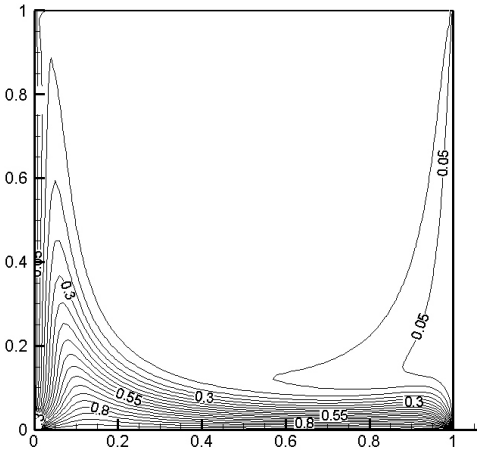

Figure 24. Dimensionless temperature contour for CMC fluid in Ri = 0.01.

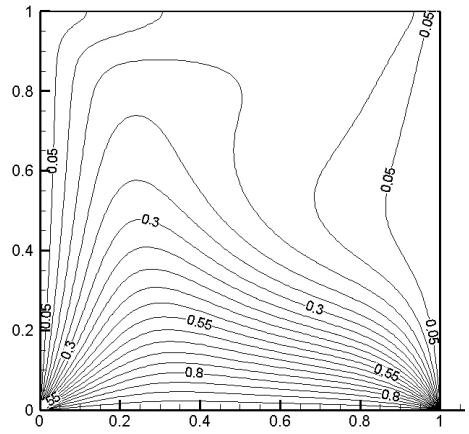

Figure 25. Dimensionless temperature contour for ideal fluid in Ri = 100.

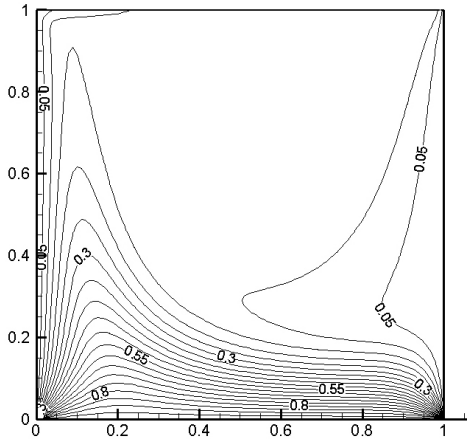

Figure 26. Dimensionless temperature contour for ideal fluid in Ri = 1.

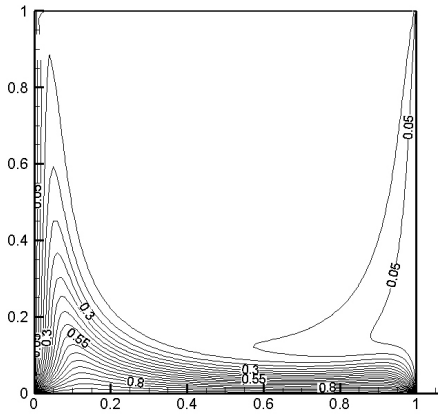

Figure 27. Dimensionless temperature contour for ideal fluid in Ri = 0.01.

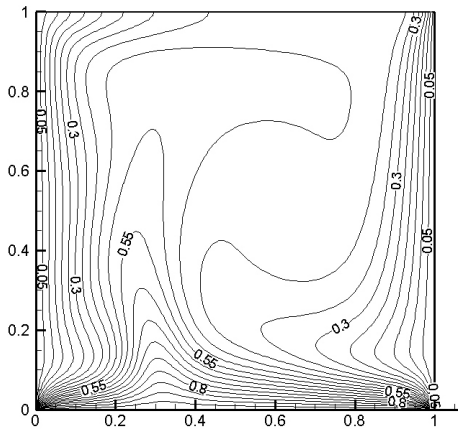

Figure 28. Dimensionless temperature contour for water in Ri = 100.

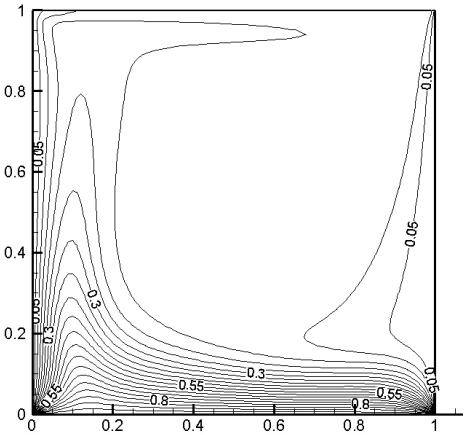

Figure 29. Dimensionless temperature contour for water in Ri = 1.

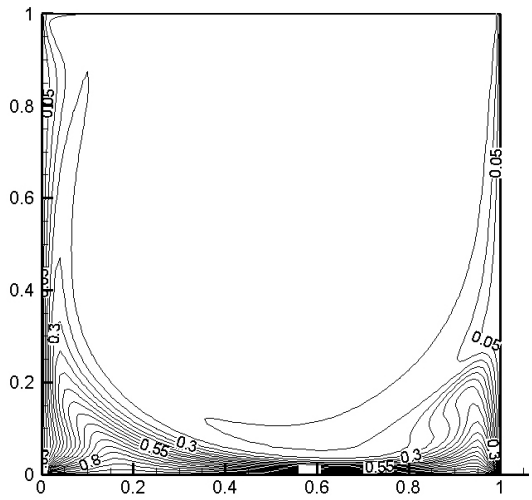

Figure 30. Dimensionless temperature contour for water in Ri = 0.01.

coupled with stream function and this is why the isothermal lines gradually become asymmetric.

It was found from Ri = 0.01 contours that due to increase in Reynolds number (Re) value and the inertia effect, the isothermal lines are pushed towards the lower and left walls. This may be described in another way similar to the one presented in Basak et al. (2009). “Because of increased recirculation and thermal mixing in the right half, the isothermal lines are pushed towards the left wall which leads in asymmetry of isothermal lines in forced convection.”

It was understood from the aforementioned contours that the temperature in the lower corners is very high and as much as we move towards the center of the enclosure, the temperature decreases which causes the increase of heat transfer rate near the lower wall and decrease in the middle of the enclosure.

Figures 31 to 47 demonstrate the contours of stream function for different non-Newtonian fluids and Richardson numbers of 0.01,1 and 100.

Considering the fact that Gr is constant in all the cases and Reynolds number changes for altering Richardson number, it may be said that “if Grashof number (Gr) is constant, increase in Re causes the augmentation of the fluid recirculation power”.

The full analysis of flow model indicates that governing mixed convection heat transfer on the enclosure is determined by two parameters of Ri and Pr. It is worthy to be noted that Prandtl number for non-Newtonian fluids is defined as follows:

$$\Pr = \frac{\left(\frac{m}{\rho}\right)^{\frac{1}{2-n}} H^{\frac{2(1-n)}{2-n}}}{k} \quad (59)$$

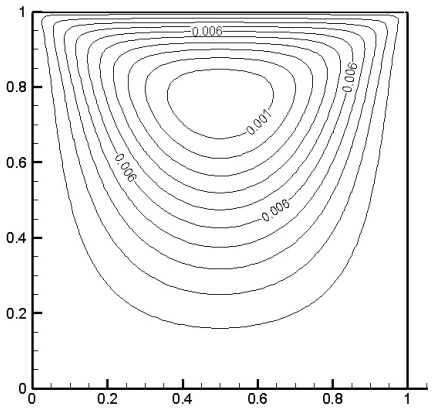

Figure 31. Stream function contour for Carbopol 0.05% fluid in Ri = 100.

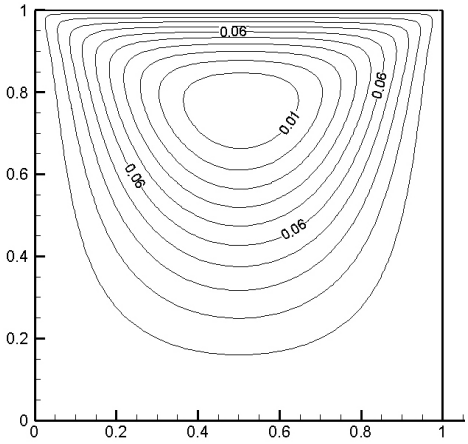

Figure 32. Stream function contour for Carbopol 0.05% fluid in Ri = 1.

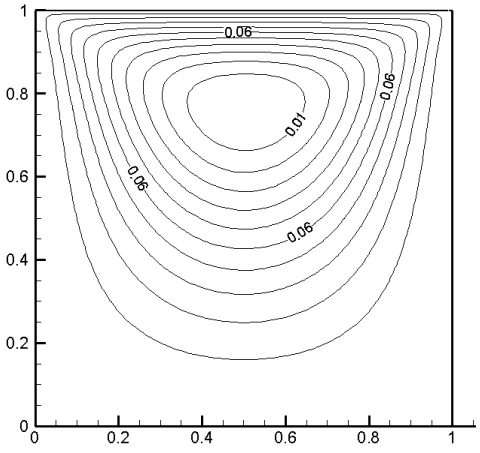

Figure 33. Stream function contour for Carbopol 0.05% fluid in Ri = 0.01.

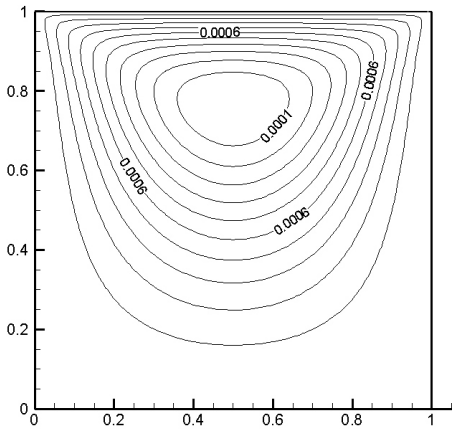

Figure 34. Stream function contour for Carbopol 0.09% fluid in Ri = 100.

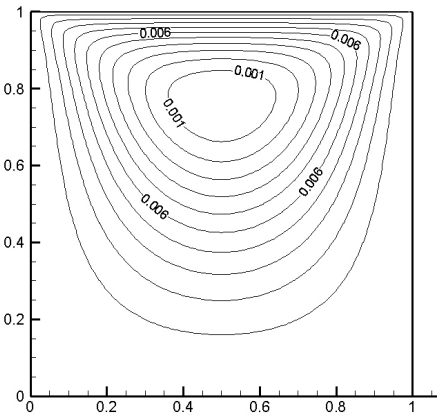

Figure 35. Stream function contour for Carbopol 0.09% fluid in Ri = 1.

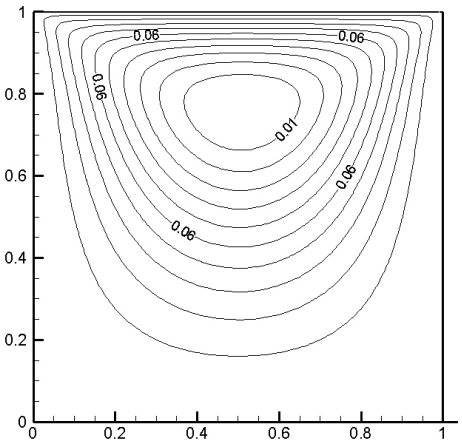

Figure 36. Stream function contour for Carbopol 0.09% fluid in Ri = 0.01.

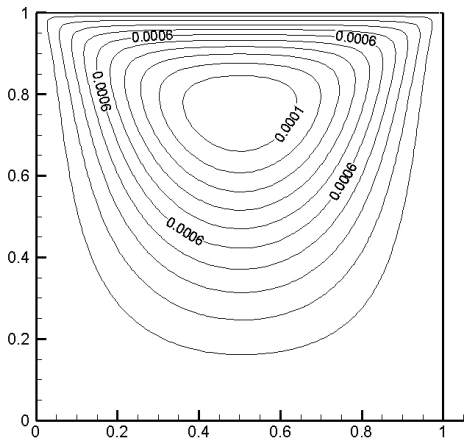

Figure 37. Stream function contour for Carbopol 0.125% fluid in Ri = 100.

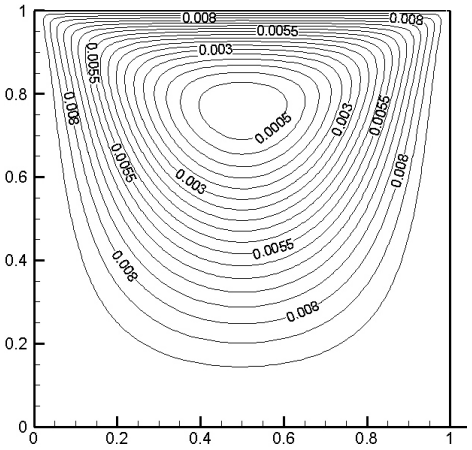

Figure 40. Stream function contour for CMC in Ri = 1.

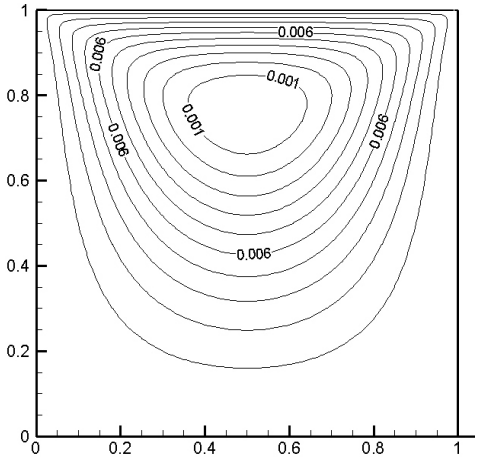

Figure 38. Stream function contour for Carbopol 0.125% fluid in Ri = 0.01.

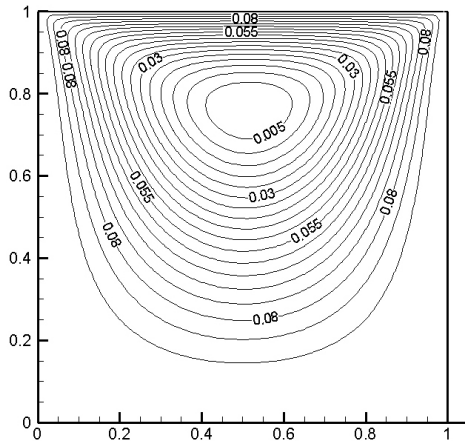

Figure 41. Stream function contour for CMC in Ri = 0.01.

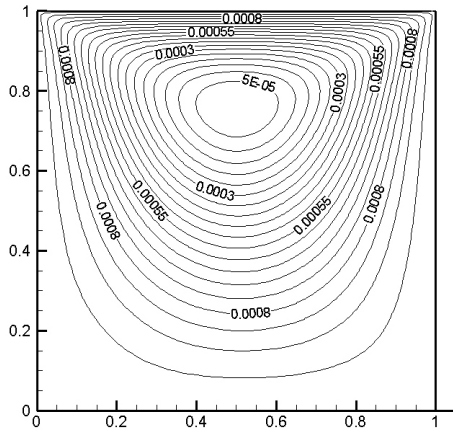

Figure 39. Stream function contour for CMC in Ri = 100.

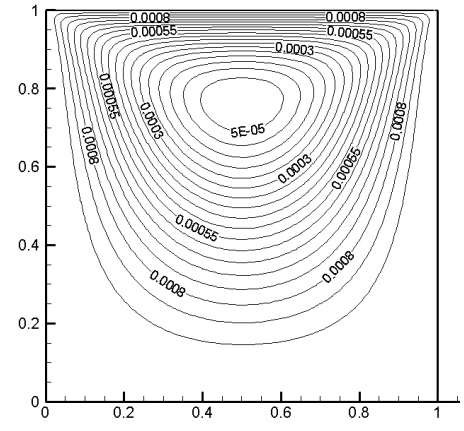

Figure 42. Stream function contour for ideal fluid in Ri = 100.

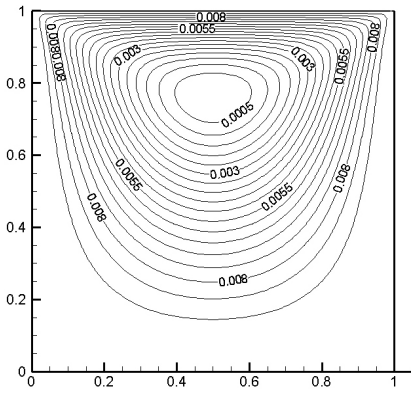

Figure 43. Stream function contour for ideal fluid in Ri = 1.

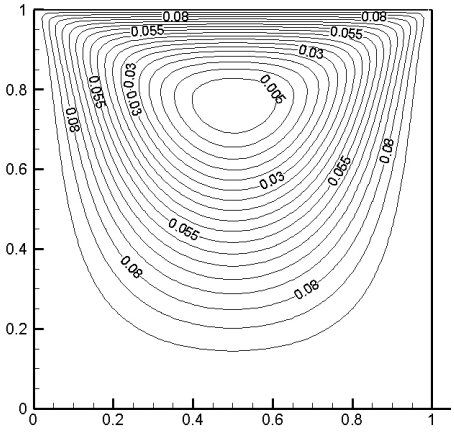

Figure 44. Stream function contour for ideal fluid in Ri = 0.01.

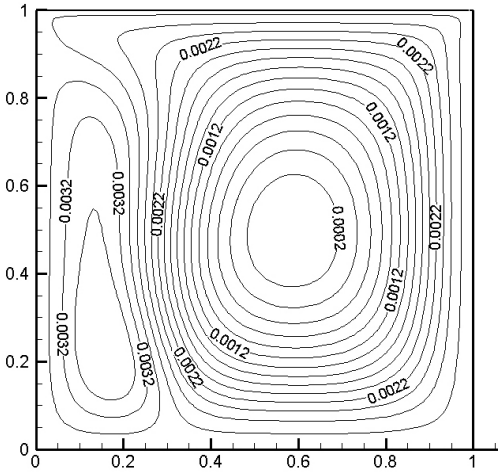

Figure 45. Stream function contour for water in Ri = 100.

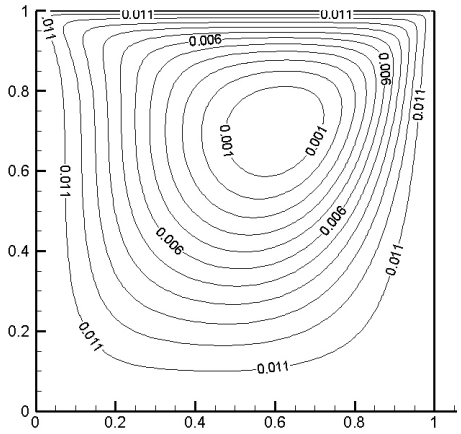

Figure 46. Stream function contour for water in Ri = 1.

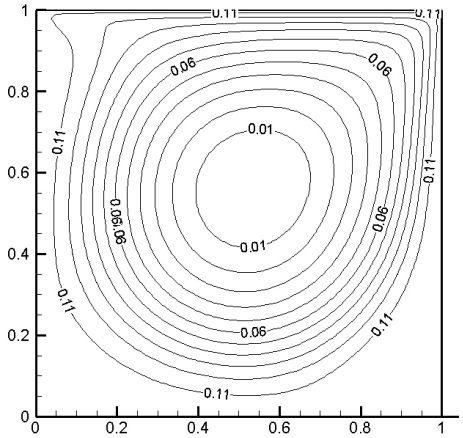

Figure 47. Stream function contour for water in Ri = 0.01.

It should be reminded that if Ri = 0.01, the power of clockwise recirculation is much more than counter-clockwise because of the high influence of the upper insulated moving wall on the flow nature. But when the effect of the velocity of the upper wall decreases, the power of clockwise flow is reduced and this will cause less power of the flow. This is why the stream function magnitude for governing forced convection is about 10 folds of the mixed convection and about 100 folds of governing natural convection, except in some exceptions.

It is necessary to be noted that the compression of stream function lines and higher digits written on them in the aforementioned contours indicate that the flows in the corresponding points for different fluids are stronger. The simultaneous influence of n and m on Pr and Gr (Ra) and the effect of Ri on flow properties have made the analysis of the earlier-stated contours very complicated nearly

impossible. Rayleigh number which is the product of Grashof number multiplied in Prandtl number is defined in non-Newtonian fluids as follows (Kim et al., 2003):

$$Ra = Gr.\Pr = \frac{g\beta\Delta T H^{3}}{k\left(\frac{m}{\rho}\right)^{\frac{1}{2-n}} H^{\frac{2(1-n)}{2-n}}} \quad (60)$$

Considering the Equation 60, we may realize the dependence of flow to Pr, Ra, n, m and Re.
In this state, the Reynolds number is defines as follows:

$$\mathrm{Re} = \frac{\rho V^{2-n} H^{n}}{m} \quad (61)$$

where, V is the velocity of moving wall of the enclosure.

For example, we may refer to the assumptive fluid (n = 1, m = 1) and CMC (n = 0.95, m = 0.044) that have the same values as the stream function. But for Carbopol fluid with different concentrations, although for concentrations such as 0.125% (n = 0.32, m = 6.67) and 0.09% (n = 0.44, m = 2.37), the values of stream function are equal but the values of stream function for the concentration of 0.05% (n = 0.65, m = 0.1103) is different from the other two fluids. Although, the apparent shapes of all stream functions are similar to each other, the only exception is water the behavior of which is near to air when compared with the non-Newtonian fluids studied in this paper.

Conclusions

In the present study, laminar mixed convection heat transfer inside a square enclosure for power-law non-Newtonian fluids like CMC and Carbopol was solved by finite volume method. Grashof number is constant (10^4) and Ri changes between 0.01 to 100. Prandtl, Grashof and Reynolds numbers have been calculated in compliance with the equations of non-Newtonian fluids. Dimensionless temperature and shear stress diagrams have been illustrated for better comparison of different fluids.

According to what has been considered in this study, it can be said that:

1. In Richardson numbers less than 1, the fluid behavior into the enclosures is forced convection, and the more the Richardson number, the more powerful the heat transfer by natural convection.
2. In governing natural convection, the isothermal lines are nearly symmetric and through transiting to forced convection, these lines become asymmetric.
3. In constant Gr, increase in Re causes the enhancement of the fluid recirculation power.
4. In constant Gr, non dimensional temperature increases by decreasing n.
5. In constant n, increase in Gr leads to increasing non dimensional temperature.
6. In the same condition, increasing forced convection causes the increasing of shear stress.

Nomenclature: u,v**,** Velocities in x and y directions [m/s]; x,y**,** Cartesian coordinates [m]; P**,** pressure [N/m^2]; T**,** temperature [K]; **t,** time [s]; **g,** gravitational acceleration [m/s^2]; k**,** thermal conductivity [W/m.K]; **Re,** Reynolds number; **Ri,** Richardson number; **Gr,** Grashof number; **Nu,** Nusselt number; **Pr,** Prandtl number; **Ra,** Rayleigh number; **H,** enclosure height [m]; **n,** power index; **m,** constitutive parameter; ρ**,** density [kg/m^3]; υ**,** kinematics viscosity [m^2/s].

Subscripts: h, Hot wall; **c,** cold wall; **m,** mean.

REFERENCES

Basak T, Roy S, Sharma PK, Pop I (2009). Analysis of mixed convection flows within a square cavity with uniform and non-uniform heating of bottom wall. Int. J. Therm. Sci., 48(5): 891-912.

Chhabra RP (2007). Bubbles, drops and particles in non-Newtonian fluids. second edition, CRC Press, Taylor & Francis Group.

Demir H, Akyoldoz FT (2000). Unsteady thermal convection of a non-Newtonian fluid. Int. J. Eng. Sci., 38: 1923-1938.

Goshayeshi HR, Safaei MR, Maghmoumi Y (2009). Numerical simulation of unsteady turbulent and laminar mixed convection in rectangular enclosure with hot upper moving wall by finite volume method. The 6th Int. Chem. Eng. Cong. and Exhib. (IChEC 2009), Kish Island, Iran.

Kim GB, Hyun JM, Kwak HS (2003). Transient buoyant convection of a power-law non-Newtonian fluid in an enclosure. Int. J. Heat Mass Trans., 46: 3605-3617.

Lamsaadi M, Naimi M, Hasnaoui M (2006). Natural convection heat transfer in shallow horizontal rectangular enclosures uniformly heated from the side and filled with non-Newtonian power law fluids, Energy Convers. Manag., 47: 2535–2551.

Maghmoumi Y (2008). Numerical investigation of steady non-Newtonian flow on a flat plate. M. Sc. thesis, IAUM, Iran (in Farsi Language).

Maghmoumi Y, Alavi SMA, Safaei MR (2008). Numerical analysis of steady non-newtonian flow over a flat plate. Maj. J. Mech. Eng., 4: 21-33 (in Farsi Language).

Turan O, Chakraborty N, Poole RJ (2010). Laminar natural convection of Bingham fluids in a square enclosure with differentially heated sidewalls. J. Non-Newtonian Fluid Mech., 165: 901–913.

Oztop HF, Dagtekin I (2004). Mixed convection in two-sided lid-drive differentially heated square cavity, Int. J. Heat Mass Trans., 47: 1761-1769.

Patankar SV (1980). Numerical heat transfer and fluid flow. Hemisphere Washington.

Safaei MR (2009). The study of turbulence mixed convection heat transfer in Newtonian and non-Newtonian fluids inside rectangular enclosures in different Richardson numbers. M. Sc. thesis, IAUM, Iran (in Farsi Language).

Safaei MR, Goshayeshi HR (2010). Numerical simulation of laminar and turbulence flow of air: natural & mechanical ventilation inside a room 10th REHVA world cong. Clima 2010 Sust. Energy Use in Build., Antalya, Turkey.

Turan O, Chakraborty N, Poole RJ (2010). Laminar natural convection of Bingham fluids in a square enclosure with differentially heated sidewalls. J. Non-Newtonian Fluid Mech., 165: 901–913.